Inorganic Chemistry

Article

pubs.acs.org/IC

Calix[4]arenes of Aluminum and Gallium with Benzimidazolyl Ligands: Steric Control of the Conformation via Substitution on the Ligand

Ernesto Rufino-Felipe,[†] Miguel-Ángel Muñoz-Hernández,*[,†] Hugo F. Saucedo-Azpeitia,[‡] and Sara A. Cortes-Llamas[‡]

[†]Centro de Investigaciones Químicas, Universidad Autónoma del Estado de Morelos, Avenida Universidad 1001, Colonia Chamilpa, Cuernavaca, Morelos 62209, Mexico

[‡]Centro Universitario de Ciencias Exactas e Ingenierías, Departamento de Química, Universidad de Guadalajara, Boulevard Marcelino García Barragán 1421, Guadalajara 44430, Jalisco, Mexico

Supporting Information

ABSTRACT: Complexes $[bzimAlR_2]_4$ [bzim = benzimidazolate; R = Et (**2**), ^{i}Bu (**3**)], $[mbzimAlR_2]_4$ [mbzim = 2-methylbenzimidazolate; R = Et (**6**), ^{i}Bu (**7**)], $[dmbzimAlR_2]_4$ [dmbzim = 5,6-dimethylbenzimidazolate; R = Me (**9**), Et (**10**), ^{i}Bu (**11**)], and $[tmbzimAlR_2]_4$ [tmbzim = 2,5,6-trimethylbenzimidazolate; R = Me (**12**), Et (**13**), ^{i}Bu (**14**)] have been prepared via alkane elimination and coordinative self-assembly upon the reaction of benzimidazole ligands with aluminum alkyls in benzene, toluene, or xylene. Characterization of the complexes was achieved by spectroscopic methods, microanalysis, and X-ray crystallography of **2**, **7**, **10**, **11**, **13**, and **14**. The complexes reported herein and the aluminum and gallium analogues **1**, **4**, **5**, and **8** reported in a previous paper[1] are predominantly tetranuclear aggregates related to calix[4]arenes in which the benzimidazolyl ligands bind two metal atoms in a $\eta^1{:}\eta^1$ fashion. X-ray crystallography demonstrates that modulation of the conformation adopted by these metallacalix[4]arenes is achieved by proper substitution on the C atom at the 2 position of the benzimidazolyl ligand. An H substituent for **1**, **2**, **4**, **10**, and **11** favors a chair conformation with a small cavity and approximate C_{2h} symmetry, while a CH_3 substituent for **5**, **7**, **8**, **13**, and **14** introduces enough repulsion to switch the conformation to a 1,3-alternate or double cone with a concomitant larger cavity and approximate C_{2v} symmetry.

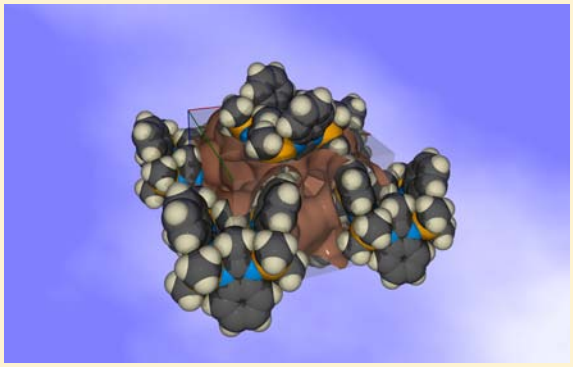

INTRODUCTION

There is considerable interest in the preparation of calixarenes[2−4] along with other classical macrocycles.[5,6] In particular, the remarkable growth of the field of calixarene chemistry has been greatly motivated by the search for derivatives capable of engaging selective complexation with neutral or ionic species.[7,8] Hoping to facilitate their synthesis and improve supramolecular properties, there has been considerable effort to modify the fundamental calixarene framework. To achieve this goal, strategies have been implemented to replace the methylene units on classical calixarenes by metals or metalloids and the phenol units by heteroaromatics using supramolecular self-assembly.[9] This is accomplished by mixing appropriate polydentate ligands with an adequate source of the metal or metalloid in solution. Examples of metallacalix[*n*]arenes have been published containing platinum $([(en)Pt(uracilate)]_4(NO_3)_4$[10] and $[Pt(thpy)(bzm)]_3)$,[11] mixed-metal metallacalix[4]arenes $[\{a_2M(N3\text{-}HC\text{-}N1)M'a'_2\}_2]^{4+}$ (a_2M = *cis*-$(NH_3)_2Pt^{II}$, a'_2M' = $(bpy)Pd^{II}$, HC = cytosine anion, bpy = 2,2′-bipyridine)[12] and *cis*-$[a_2M(cytosine\text{-}N3)_2]^{2+}$ (M = Pt^{II}, Pd^{II}; *n* = 4 and 6),[13] rhenium $[\{(CO)_3Re\}_4(L)_2(4,7\text{-phen})_2$ (L = 1,2,4-trihydroxy-9,10-anthraquinone (thaq)],[14] and iron ($[Fe(NO)_2(Im\text{-}H)]_4$).[14] Boron calix[3,4,5]arenes[15−18] derived from imidazole, benzimidazole, and salicylaldehyde are known. However, the synthesis of metallacalixarenes derived from the heavier group 13 elements has received much less attention, so far. Recently, our research group reported the straightforward preparation of four metallacalix[4]arenes derived from $AlMe_3$ and $GaMe_3$ with benzimidazolate (bzim) and 2-methylbenzimidazolate (mbzim) ligands at room temperature in benzene (Figure 1).[1]

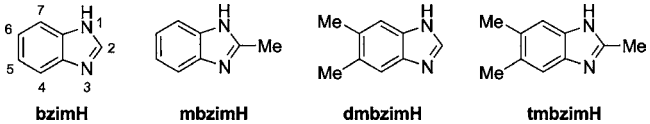

Figure 1. Proligands used to obtain aluminum and gallium calix[4]arenes.

Received: August 3, 2012
Published: November 13, 2012

   dx.doi.org/10.1021/ic301718m | *Inorg. Chem.* 2012, 51, 12834−12840

Metallacalix[4]arenes $[bzimAlMe_2]_4$ (**1**), $[bzimGaMe_2]_4$ (**4**), $[mbzimAlMe_2]_4$ (**5**), and $[mbzimGaMe_2]_4$ (**8**), afforded via the coordination of four 150° edges provided by the benzimidazolyl ligands and four ditopic tetrahedral binding sites of ca. 109° provided by $AlMe_2$ or $GaMe_2$ moieties as a result of alkane elimination, show steric control of the conformation of the resultant metallacycles by proper substitution on the C atom at the 2 position of the benzimidazolyl ligand. An H substituent on **1** and **4** favors the chair conformation and approximate C_{2h} symmetry with a small cavity, while a CH_3 substituent on **5** and **8** introduces enough steric repulsions to switch the conformation to 1,3-alternate with C_{2v} symmetry and a concomitant larger cavity.

Complexes **1** and **4** do not include solvent in their cavities or in the crystal lattice. By contrast, **5** and **8** show an arrangement of alternating columns of complex-included and crystallization solvents. Furthermore, evidence of the formation of pentanuclear metallacycles $[mbzimAlMe_2]_5$ and $[mbzimGaMe_2]_5$ as minor products (less than 10%) for **5** and **8** was attained by mass spectrometry (M^+ at m/z 940 and 1150, respectively) and ^{1}H NMR spectroscopy.

In the following, we report investigations on aluminum calix[4]arenes derived from bzim ligands with methyl substituents on different parts of the ligand (Scheme 1). The report is focused on the effect of the substituent on the Al center, the guest properties of aromatic solvents with different sizes used as reaction media, and their role on the final crystal structure.

Scheme 1. Aluminum and Galliumcalix[4]arenes 1, 4, 5, and 8 Reported in a Previous Paper[1]

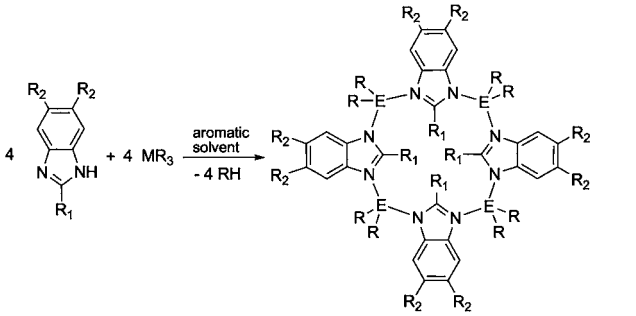

RESULTS AND DISCUSSION

Following the procedures described previously for **1**, **4**, **5**, and **8**,[1] complexes **2**, **3**, **6**, **7**, and **9**−**14** were prepared in high yields by one-step syntheses by reacting proligands bimH, mbimH, dmbimH, and tmbimH with aluminum alkyls, AlR_3, at ambient temperature in benzene, toluene, or *p*-xylene, as shown in Scheme 1. All complexes are air-sensitive white solids. However, under argon, they are stable in the solid state and in solution for several days at ambient temperature.

The IR spectra of these complexes do not show the typical absorption band around 3400 cm^{-1} related to the stretching of the N−H bond of proligands, furnishing evidence that a metalation reaction indeed occurred. ^{1}H and ^{13}C NMR in solution show that the complexes investigated are obtained as single species, presumably tetranuclear aluminum calix[4]-arenes. As a consequence, the ^{1}H NMR spectra in chloroform-d_1 show only one set of resonance signals for the protons linked to the benzimidazolyl moieties as well as one set of signals at high field assigned to the aluminum alkyl protons. The latter chemical shifts are in the range observed for other reported aluminum alkyl complexes.[19] A similar trend is observed in the ^{13}C NMR spectra (Figures S8−S27 in the Supporting Information). In the previous report, the evidence provided by NMR and mass spectrometry supported the formation of the pentanuclear species $[mbzimAlMe_2]_5$ and $[mbzimGaMe_2]_5$ as minor products during the synthesis of **5** and **8** in benzene solutions.[1] This is not the case for any of the complexes disclosed on this report even using toluene for **7** and **14** or *p*-xylene for **2** as reaction media, which may induce a template effect.[20]

X-ray crystallography confirmed for **2**, **7**, **10**, **11**, **13**, and **14** the formation of exclusively tetranuclear species. Table S1 in the Supporting Information gives relevant data of the crystal collection, and Table 1 lists selected bond lengths and angles. The molecular structures of the representative complexes **10** and **13** are shown in Figures 2 and 3, respectively. The structures of complexes **2**, **7**, **11** and **14** are included in Figures S1−S6 in the Supporting Information. The molecular

Table 1. Selected Bond Lengths (Å) and Angles (deg) for Complexes 2, 7, 10, 11, 13, and 14

2				**7**			
Al1−N1	1.926(4)	N1−Al1−N3	98.6(2)	Al1−N1	1.950(3)	N1−Al1−N8	101.8(1)
Al1−N2	1.940(4)	N1−Al1−C15	109.9(2)	Al2−N3	1.954(3)	C33−Al1−C37	122.3(2)
Al1−C15	1.963(4)	N3−Al1−C17	108.2(2)	Al1−C33	1.992(4)	N1−Al1−C33	110.4(2)
Al1−C17	1.986(5)	C15−Al1−C17	120.9(2)	Al2−C45	1.978(4)	N8−Al1−C33	104.5(2)
10				**11**			
Al1−N1	1.939(3)	N1−Al1−N5	99.0(2)	Al1−N1	1.936(4)	N1−Al1−N8	96.7(2)
Al1−N5	1.944(4)	N1−Al1−C23	109.4(2)	Al1−N8	1.937(4)	N1−Al1−C37	110.3(2)
Al1−C23	1.961(4)	N1−Al1−C25	107.2(2)	Al1−C37	1.969(5)	N1−Al1−C41	107.5(2)
Al1−C25	1.968(5)	N5−Al1−C25	108.7(2)	Al1−C41	1.969(5)	N8−Al1−C41	107.5(2)
13				**14**			
Al1−N1	1.939(4)	N1−Al1−N8	103.0(2)	Al1−N1	1.950(4)	N1−Al1−N8	103.8(2)
Al1−N8	1.935(4)	N1−Al1−C41	105.0(2)	Al1−N8	1.955(4)	N1−Al1−C41	102.8(2)
Al1−C41	1.967(5)	N1−Al1−C43	109.9(2)	Al1−C41	1.983(5)	N1−Al1−C45	111.3(2)
Al1−C43	1.957(5)	N8−Al1−C41	105.0(2)	Al1−C45	1.980(5)	N8−Al1−C41	109.4(2)

dx.doi.org/10.1021/ic301718m | *Inorg. Chem.* 2012, 51, 12834−12840

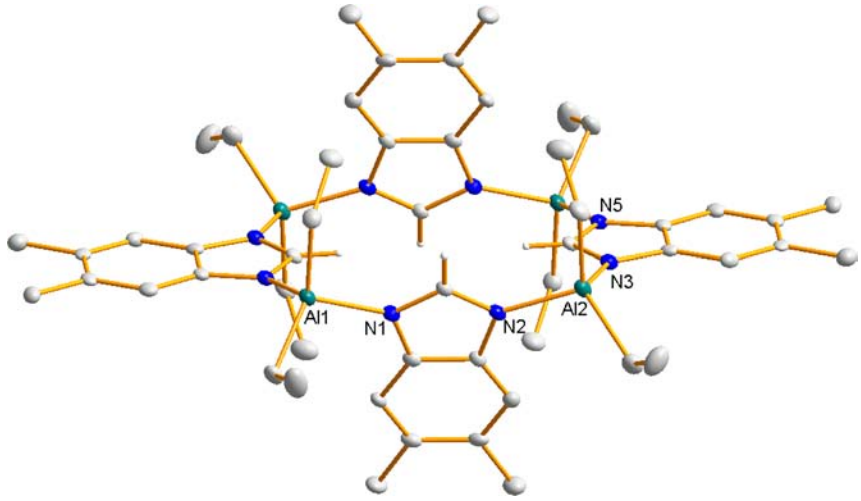

Figure 2. Molecular structure of **10** showing thermal ellipsoids at the 30% level, with most H atoms omitted for clarity.

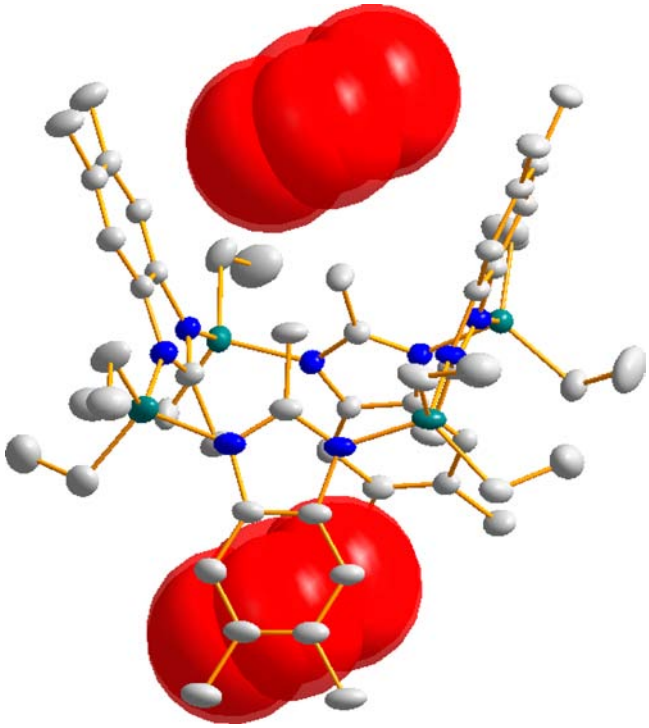

Figure 3. Molecular structure of **13** showing thermal ellipsoids at the 30% level and including benzene molecules in the space-filling representation. H atoms have been omitted for clarity.

structures show 16-membered macrocycles with the benzimidazolyl ligands coordinated in a η^1:η^1 fashion and bridging two Al centers. Steric control of the conformation of the 16-membered metallacycles is achieved by proper substitution on the C atom at the 2 position of the benzimidazolyl ligand, as was observed in the previous report for complexes **1**, **4**, **5**, and **8**. An H substituent for **2**, **10**, and **11** favors the C_{2h}-symmetric complexes, while a CH_3 substituent for **7**, **13**, and **14** introduces enough repulsion to switch the conformation to the C_{2v}-symmetric complexes.

The solvent-accessible volume of the cavities for complexes with a chair conformation (**1**, **2**, **4**, **10**, and **11**) was calculated by assuming a spherical shape of $V = (4/3)\pi r^3$ (Table 2a). The sphere was outlined with the two proximal H atoms in the 2

Table 2. Total Volume of Cavities for Complexes with Chair Conformation [$V = (4/3)\pi r^3$] and 1,3-Alternating Conformation ($V = 2[(1/3)\pi h(a^2 + ab + b^2)]$) and Pore Volumes (0.0003 au)

a. Complexes with C_{2h} Chair Conformation					
	1	**2**	**4**	**10**	**11**
R (Å)	0.80	0.78	0.85	0.79	0.83
volume of the cavity (Å^3)	2.2	2.0	2.6	2.1	2.4
pore volume (cm^3 g^{-1})[a]	0.015	0.067	0.011	0.049	0.084
b. Complexes with C_{2v} 1,3-Alternating Conformation					
	5	**7**	**8**	**13**	**14**
a (Å)	3.54	3.40	3.66	3.64	3.66
b (Å)	0.10	0.17	0.07	0.12	0.16
h (Å)	6.75	6.76	6.76	7.78	7.77
total volume of the cavities (Å^3)	183	173	195	224	229
pore volume (cm^3 g^{-1})[a]	0.239	0.098	0.285	0.122	0.146

[a]The CIF files were modified by removing solvent molecules in order to map the void space.

position of the benzimidazolyl ligands (Figure S7 in the Supporting Information). For macrocycles with a 1,3-alternate conformation (**5**, **7**, **8**, **13**, and **14**), the total available volume was calculated by approximating the shape of the cavities to truncated cones of $V = [(1/3)\pi h(a^2 + ab + b^2)]$ (Table 2b). The centroid of the H atoms or the H atoms on the methyl groups in the 5 and 6 positions for mutually *syn*-mbzim and tmbzim ligands, respectively, delimit the larger circumference (a), the H atoms of a methyl substituent in the 2 position delimit the shorter circumference (b), and the height (h) is the distance between a and b (Figure S7 in the Supporting Information). To determine a more realistic solvent-accessible volume of the cavities, the van der Waals radii of the atoms implied in the calculations were taken into account. The mapping of the void space using the procrystal electron density with 0.0003 au isosurfaces implemented in *CrystalExplorer* was also used to estimate the solvent-accessible volume of the cavities and channels in the crystal structures (Table 2).[21] The use of the 0.0003 au isovalue has been demonstrated to be the best choice for exploring porous materials with permanent voids like covalent organic frameworks (COFs) and metal-loorganic frameworks.[22]

dx.doi.org/10.1021/ic301718m | *Inorg. Chem.* 2012, 51, 12834−12840

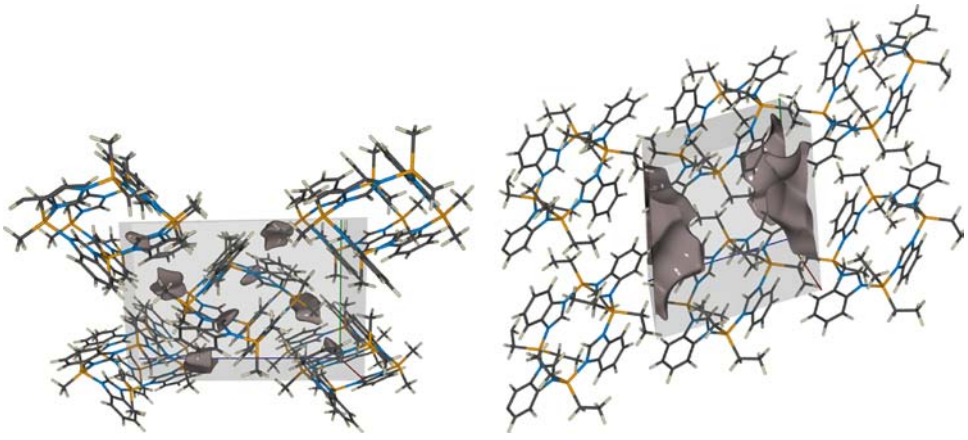

Figure 4. Void surfaces for **1** and **2** at 0.0003 au with molecules in a wire/stick representation and the unit cell in gray. The view is down the *a* axis.

The very small cavity volumes of complexes in the chair conformation do not allow access of the guest molecules, although *p*-xylene is found to occupy voids in the crystal structure of **2** and benzene in **10** and **11**. The aluminum and gallium complexes **1** and **4** with the smallest benzymidazolate ligand, bzim, and the shortest alkyl group on the metal center, methyl (Me), pack in such a way that interactions between tetrametallic complexes are maximized through a network of hydrogen bonds of the type $AlCH_2$–H···HCBz (3.59–3.83 Å) and layer stacking with $\pi\cdots\pi$ (4.11–4.95 Å) and C–H···π (3.56–3.59 Å) interactions, which altogether minimizes the void space.[1] The introduction of a longer ethyl (Et) substituent on aluminum for **2** favors the formation of voids in the crystal structure that are filled with *p*-xylene (Figure 4). Accordingly, **11** with isobutyl (^{i}Bu) substituents on aluminum and the dmbzim ligand show the biggest pore size of 0.084 $cm^3\ g^{-1}$ for this series, which allows two molecules of benzene in the unit cell. The interactions that sustain the crystal lattice in **2**, **10**, and **11** are $\pi\cdots\pi$ and CH···π type in nature. For example, in **10**, the unit cell contains two molecules of the macrocycle and two molecules of benzene; its crystal packing shows an arrangement of alternating columns of complex benzene along the *bc* plane through $\pi\cdots\pi$ *face-to-face-stacked* interactions of ≈3.9 Å between benzene and the six-membered ring of the dmbzim ligand (Figure 5). In addition, the methylene groups of the Et substituent on the Al center establish CH···π interactions of ≈3.7 Å with the six-membered ring of the dmbzim ligand of adjacent tetramers. Such $\pi\cdots\pi$ interactions have been the subject of intensive studies because of their strong influence in the determination of the structure, stability, and crystal packing of the systems in which they intervene.[23−26]

The larger cavity size in the range of 173–229 $Å^3$ for the C_{2v} aluminum calix[4]arenes **5**, **7**, **8**, **13**, and **14** allows the inclusion of at least one solvent molecule per macrocycle, via CH···π interactions (3.46–4.53 Å). **7** includes one molecule of toluene, while **13** and **14** include two molecules of benzene and toluene, respectively (Figures S2 and S5 in the Supporting Information and Figure 3). The previously reported complexes **5** and **8** include four molecules of benzene.[1] Although **13** and **14** show a considerably larger cavity than **5**, **7**, and **8** (Table 2b), the presence of bigger alkyl groups on the Al center prevents further inclusion of a solvent in their cavities. An additional effect in **13** that precludes the inclusion of more solvent is the Me substituent in the 5 and 6 positions on the tmbzim ligand, which promote interpenetration of aluminum calix[4]arene

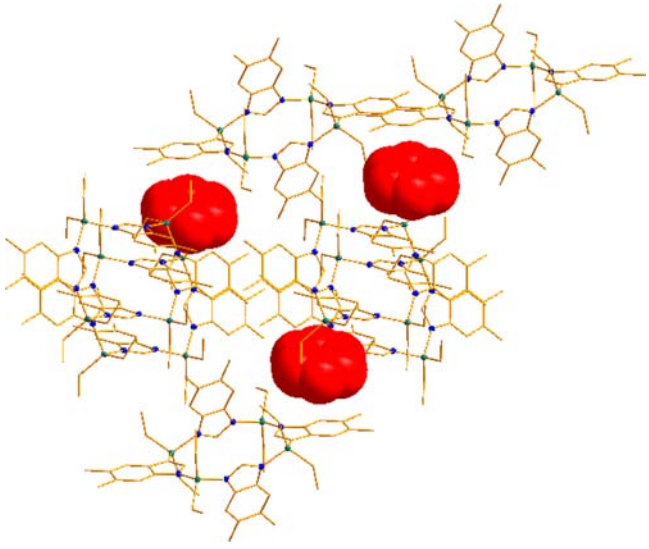

Figure 5. Crystal structure of **10** in a wire/stick representation and benzene solvate molecules in the space-filling style. H atoms have been omitted for clarity.

molecules in an almost *head-to-tail* arrangement through C–$H_{methyl}\cdots\pi$ interactions (4.16–4.37 Å), forming columns that run along the *c* axis (Figure 6). **7** includes less solvent than **5** and **8** because of the larger size of toluene compared to benzene and the longer ^{i}Bu than Me, which blocks access of the solvent to the cavity (Figure 7). For **13**, included benzene is bound to the macrocycle through CH···π interactions that connect C–$H_{benzene}$ with a six-membered ring of the ligand (≈3.6 Å). The metallacycles interact through CH···π bonding of ≈3.5 Å with CH_3 of the Et substituent on the Al center and the six-membered ring of the tmbzim ligand. In addition, two sets of benzene molecules stack along the *c* axis, and they interact with the tetramers through CH···π interactions with the Et groups on the Al centers. The crystal structures of **7** and **14** are less ordered because of the presence of 2_1 screw axes and glide planes in both cases, but the interactions are similar to those described for **13** (Figures S3 and S6 in the Supporting Information). Table 2b suggests that the pore volumes are maximized for complexes with the shortest alkyl on the metal center and smallest ligand (**5** and **8**), or in other words, the metallacycle has to be as simple as possible to create more voids in the crystal lattice. The introduction of longer alkyl

dx.doi.org/10.1021/ic301718m | *Inorg. Chem.* 2012, 51, 12834–12840

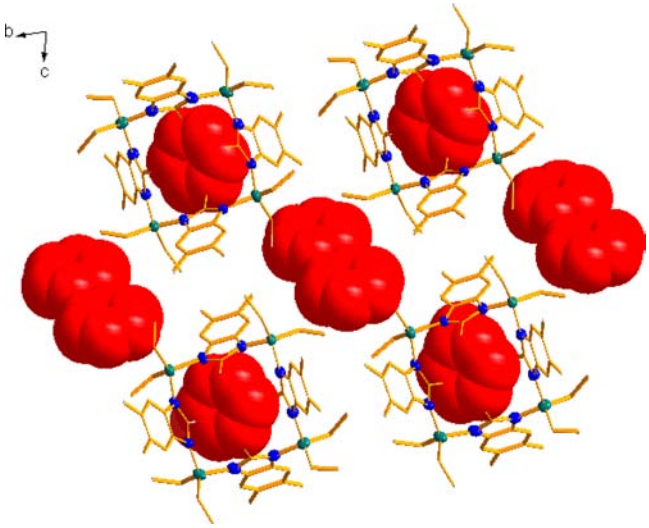

Figure 6. Crystal structure of **13** in a wire/stick representation and benzene solvate molecules in the space-filling style. H atoms have been omitted for clarity.

substituents on the metal center block access to the cavities, and the presence of additional Me groups on the ligand promotes interpenetration of metallacycles filling voids in the crystal lattice and blocking access of the solvent. The porosities observed for **5** and **8** of 0.239 and 0.285 $cm^3\ g^{-1}$, respectively, are remarkably similar to those observed for the 2D COFs; COF-1 and COF-6 (0.231 and 0.289 $cm^3\ g^{-1}$), of ref 22.

CONCLUSIONS

The reaction of various benzimidazole-based ligands with aluminum or gallium alkyls leads to the formation of tetrametallic products preferentially over higher aggregates. Steric control of the conformation of the 16-membered metallacycles is achieved by proper substitution on the C atom at the 2 position of the benzimidazolyl ligand. An H substituent favors a chair conformation with a small cavity and approximate C_{2h} symmetry, while a CH_3 substituent introduces enough repulsion to switch the conformation to 1,3-alternate or double cone with a concomitant larger cavity and approximate C_{2v} symmetry. For complexes with chair conformation, the crystallization solvent is not included in the small cavities, although the solvent can fill voids in the crystal lattice for complexes with long alkyl substituents on the metal center. Because of the larger cavity size, complexes with 1,3-alternating conformation include in their cavities at least one solvent molecule and no more than four through CH$\cdots\pi$ interactions. The host properties of these complexes improve with short substituents on the metal center, while bigger solvent guest molecules than benzene allow the inclusion of no more than two solvent molecules. The formation of channels in the crystal structure of these isomers is also favored with short substituents on the metallic center and with small benzimadazolate ligands. The porosity of the aluminum and gallium calix[4]arene crystals **5** and **8** is remarkably comparable to that of 2D COFs. Future research will target the preparation of more robust to air metal or metalloid calix[4]arenes using the mbzim ligand.

EXPERIMENTAL SECTION

General Procedures. All experiments were carried out under argon using standard Schlenk techniques in conjunction with an inert-atmosphere glovebox. Toluene, benzene, and hexane were dried with a MBraun solvent purifier. *p*-Xylene was distilled from sodium/benzophenone and stored under argon prior to use. 2-Methylbenzimidazole (mbzimH) and 2,5,6-trimethylbenzimidazole (tmbzimH) were prepared as described in the literature.[27] All chemicals were purchased from Aldrich and used as received. ^{1}H and ^{13}C NMR spectra were recorded on a Varian Gemini 200 MHz spectrometer (200 MHz for ^{1}H and 50.30 MHz for ^{13}C) at ambient probe temperature (293 K). ^{1}H and ^{13}C NMR chemical shifts were determined by reference to residual solvent signals. IR data were recorded as KBr pellets on a Bruker Vector 22 FT-IR spectrometer and are reported in cm^{-1}. Melting points were measured in a Mel Temp II device using sealed capillaries and are uncorrected. Elemental analyses (C, H, and N) were carried out with a Vario EL III elementar analyzer.

Single-Crystal X-ray Crystallography. X-ray data for **2**, **7**, **10**, **11**, and **13**–**16** were collected using the program *SMART*[28] on a Bruker APEX CCD diffractometer with monochromatized Mo Kα radiation (λ = 0.71073 Å). Cell refinement and data reduction were carried out using the program *SAINT*; the program *SADABS* was employed to make incident beam, decay, and absorption corrections in the *SAINT-Plus*, version 6.0, suite.[29] Then, the structures were solved by direct methods with the *SHELXS* program and refined by full-

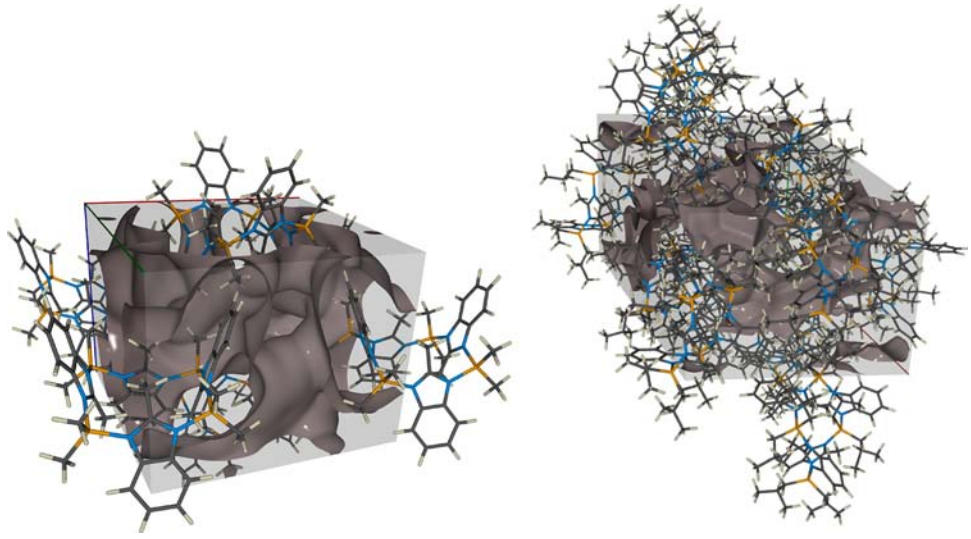

Figure 7. Void surfaces for **5** and **7** at 0.0003 au with molecules in a wire/stick representation and the unit cell in gray down the *b* axis.

dx.doi.org/10.1021/ic301718m | *Inorg. Chem.* 2012, 51, 12834–12840

matrix least-squares techniques with *SHELXL* in the *SHELXTL*, version 6.1, suite.[30] Crystals of **7** show two molecules of toluene in the asymmetric unit on a σ crystallographic plane. One molecule was refined by taking into account half-occupancy for the Me substituent on the aromatic ring, and the other molecule was refined into two split positions, giving an occupancy factor level of 0.48. Constraints and restraints were used in all of the models to obtain the best possible anisotropic displacement parameters for the C atoms. H atoms were generated in calculated positions and constrained with the use of a riding model. The final models involve anisotropic displacement parameters for all non-H atoms. Further details of the structure analyses are given in Table S1 in the Supporting Information and Tables 1 and 2. Crystal structures were analyzed and figures were prepared using the software suites *Diamond 3.0*,[31] *Mercury 3.0*,[32] *POV-Ray 3.6*,[33] and *CrystalExplorer 3.0*.

Synthesis of Aluminum Calix[4]arenes. *[(μ^1,μ^1-bzim)(μ-Al)Et$_2$]$_4$ (**2**).* A solution of AlEt$_3$ (0.21 g, 1.82 mmol) in 15 mL of *p*-xylene was slowly added to a stirred solution of benzimidazole (0.2 g, 1.69 mmol) in 15 mL of toluene. The reaction mixture was stirred for 6 h at ambient temperature, concentrated. and stored at −20 °C. Once the compound crystallized, it was isolated by cannula filtration and dried under dynamic vacuum. Yield: 0.24 g, 70%. ^{1}H NMR (CDCl$_3$): δ 7.5 (m, 2H, Ar−*H*), 7.3 (s, 1H, Ar−*H*), 6.9 (m, 2H, Ar−*H*), 1.14 (t, 6H, Al−CH$_2$C*H*$_3$), 0.48 (q, 4H, Al−C*H*$_2$CH$_3$). ^{13}C NMR (CDCl$_3$): δ 148, 138, 124, 116, 9.1, 0.3. IR (ν_{max}/cm^{-1}): 3060.2 (w), 2934.3 (s), 2897.7 (s), 2860.6 (s), 2789.7 (w), 1612.3(w), 1491.4 (s), 1461.0 (s), 1409.7 (m), 1347.1 (w), 1301.5 (m), 1272.2 (s), 1246.7 (s), 1182.8 (w), 1119.8 (m), 1040.7 (w), 1010.9 (w), 986.7 (m), 776.1 (w), 745.8 (s), 660.8 (s), 616.8 (m), 583.3 (w), 551.5 (w). Anal. Calcd for C$_{44}$H$_{60}$N$_8$Al$_4$: C, 65.33; H, 7.48; N, 13.85. Found: C, 65.05; H, 7.36; N, 13.47.

*[(μ^1,μ^1-bzim)(μ-Al)^{i}Bu$_2$]$_4$ (**3**).* A solution of Al^{i}Bu$_3$ (0.46 g, 1.82 mmol) in 15 mL of toluene was slowly added to a stirred solution of benzimidazole (0.2 g, 1.69 mmol) in 15 mL of toluene. The reaction mixture was stirred for 6 h at ambient temperature, concentrated, and stored at −20 °C. Once the compound crystallized, it was isolated by cannula filtration and dried under dynamic vacuum. Yield: 0.35 g, 82%. Mp: 189−194 °C. ^{1}H NMR (CDCl$_3$): δ 7.60 (s, 1H, Ar−*H*), 7.56 (m, 2H, Ar−*H*), 6.98 (m, 2H, Ar−*H*), 1.89 (m, 2H, Al−CH$_2$C*H*(CH$_3$)$_2$, 0.98 (d, 12H, Al−CH$_2$CH(C*H*$_3$)$_2$, 0.66 (d, 4H, Al−C*H*$_2$CH(CH$_3$)$_2$. ^{13}C NMR (CDCl$_3$): δ 147.8, 138.9, 124.3, 116.0, 28.32, 26.44, 22.1. IR (ν_{max}/cm^{-1}): 2949.4 (s), 2862.6 (m), 1779.2 (w), 1613.0 (w), 1489.8 (m), 1461.3 (m), 1361.6 (w), 1321.6 (w), 1300.9 (w), 1268.4 (m), 1246.8 (m), 1179.6 (m), 1120.3 (w), 1063.6 (m), 1011.9 (m), 915.5 (m), 813 (s), 775.8 (s), 743.7 (s), 678.0 (m), 556.1 (s), 478.3 (s), 428.7 (m). Anal. Calcd for C$_{60}$H$_{92}$N$_8$Al$_4$: C, 69.74; H, 8.97; N, 10.84. Found: C, 69.48; H, 8.42; N, 10.75.

*[(μ^1,μ^1-mbzim)(μ-Al)Et$_2$]$_4$ (**6**).* A solution of AlEt$_3$ (0.30 g, 2.62 mmol) in 15 mL of toluene was slowly added to a stirred solution of methylbenzimidazole (0.3 g, 2.27 mmol) in 15 mL of toluene. The reaction mixture was stirred for 24 h at ambient temperature, concentrated, and stored at −20 °C. Once the compound crystallized, it was isolated by cannula filtration and dried under dynamic vacuum. Yield: 0.42 g, 80%. Mp: 210 °C. ^{1}H NMR (CDCl$_3$): δ 7.75 (m, 2H, Ar−*H*), 7.26 (m, 2H, Ar−*H*), 1.82 (s, 3H, Ar−C*H*$_3$), 0.91 (t, 6H, Al−CH$_2$C*H*$_3$), 0.42 (q, 4H, Al− C*H*$_2$CH$_3$). ^{13}C NMR (CDCl$_3$): δ 158.21, 139.70, 123.48, 115.29, 15.46, 8.64, 1.75. IR (ν_{max}/cm^{-1}): 3060.27 (w), 2950.30 (s), 2870.43 (m), 2792.76 (w), 2607.45 (w), 2374.96 (w), 1606.27 (w), 1452.81 (s), 1399.29 (s), 1323.95 (w), 1268.34 (m), 1176.88 (w), 1061.08 (m), 1019.43 (m), 923.94 (w), 862.91 (w), 809.23 (w), 745.65 (m), 681.27 (m), 490.97 (w). Anal. Calcd for C$_{48}$H$_{68}$N$_8$Al$_4$: C, 66.65; H, 7.92; N, 12.95. Found: C, 64.85; H, 7.71; N, 12.26.

*[(μ^1,μ^1-mbzim)(μ-Al)^{i}Bu$_2$]$_4$ (**7**).* A solution of Al^{i}Bu$_3$ (0.52 g, 2.62 mmol) in 15 mL of toluene was slowly added to a stirred solution of methylbenzimidazole (0.3 g, 2.27 mmol) in 15 mL of toluene. The reaction mixture was stirred for 24 h at ambient temperature, concentrated, and stored at −20 °C. Once the compound crystallized, it was isolated by cannula filtration and dried under dynamic vacuum. Yield: 0.49 g, 75%. Mp: 205 °C. ^{1}H NMR (CDCl$_3$): δ 7.75 (m, 2H, Ar−*H*), 7.23 (m, 2H, Ar−*H*), 1.79 (s, 3H, Ar−C*H*$_3$), 1.46 (m, 2H, Al−CH$_2$C*H*(CH$_3$)$_2$, 0.71/0.85 (diasterotopic, d, 12H, Al−CH$_2$CH-(C*H*$_3$)$_2$), 0.60 (d, 4H, Al−C*H*$_2$CH(CH$_3$)$_2$. ^{13}C NMR (CDCl$_3$): δ 158.71, 139.79, 123.70, 115.79, 28.51, 27.86, 26.49, 24.43, 16.03. IR (ν_{max}/cm^{-1}): 3060.27 (w), 2950.30 (s), 2870.43 (m), 2792.76 (w), 2607.45 (w), 2374.96 (w), 1606.27 (w), 1452.81 (s), 1399.29 (s), 1323.95 (w), 1268.34 (m), 1176.88 (w), 1061.08 (m), 1019.43 (m), 923.94 (w), 862.91 (w), 809.23 (w), 745.65 (m), 681.27 (m), 490.97 (w). Anal. Calcd for C$_{64}$H$_{100}$N$_8$Al$_4$: C, 70.56; H, 9.25; N, 10.29. Found: C, 69.46; H, 9.12; N, 10.23.

*[(μ^1,μ^1-dmbzim)(μ-Al)Me$_2$]$_4$ (**9**).* A solution of Me$_3$Al (0.08 g, 1.08 mmol) in 15 mL of benzene was slowly added to a stirred solution of 5,6-dimethylbenzimidazole (0.15 g, 1.02 mmol) in 15 mL of benzene. The reaction mixture was stirred for 6 h at ambient temperature. The solution was concentrated to 10 mL and stored under argon at 4 °C. Once the compound crystallized, it was isolated by cannula filtration and dried under dynamic vacuum. Yield: 0.18 g, 88%. ^{1}H NMR (CDCl$_3$): δ 7.28 (s, 2H, Ar−*H*), 7.17 (s, 1H, Ar−*H*), 2.26 (s, 6H, Ar−C*H*$_3$), −0.50 (s, 6H, Al−C*H*$_3$). ^{13}C NMR (CDCl$_3$): δ 147.38, 137.82, 133.36, 116.03, 20.81, −9.65. IR (ν_{max}/cm^{-1}): 3400.0 (w), 2930.3 (s), 1774.3 (w), 1584.0.1 (w), 1491.2 (s), 1337.8 (w), 1255.0 (s), 1199.5 (s), 1095.6 (m), 1045.5 (m), 828.8 (m), 688.5 (s), 574.3 (m), 481.6 (m). Anal. Calcd for C$_{44}$H$_{60}$N$_8$Al$_4$: C, 65.33; H, 7.48; N, 13.85. Found: C, 64.02; H, 7.13; N, 13.22.

*[(μ^1,μ^1-dmbzim)(μ-Al)Et$_2$]$_4$ (**10**).* A solution of Et$_3$Al (0.12 g, 1.08 mmol) in 15 mL of benzene was slowly added to a stirred solution of 5,6-dimethylbenzimidazole (0.15 g, 1.02 mmol) in 15 mL of benzene. The reaction mixture was stirred for 6 h at ambient temperature. The solution was concentrated to 10 mL and stored under argon at 4 °C. Once the compound crystallized, it was isolated by cannula filtration and dried under dynamic vacuum. Yield: 0.22 g, 92%. ^{1}H NMR (CDCl$_3$): δ 7.24 (s, 2H, Ar−*H*), 7.12 (s, 1H, Ar−*H*), 2.28 (s, 3H, Ar−C*H*$_3$), 0.91 (t, 6H, Al−CH$_2$C*H*$_3$), 0.24 (q, 4H, Al−C*H*$_2$CH$_3$). ^{13}C NMR (CDCl$_3$): δ 147.74, 137.64, 133.54, 115.99, 20.76, 9.16, −0.47. IR (ν_{max}/cm^{-1}): 3425.0 (w), 3029.3 (m), 2934.0 (s), 2862.1 (s), 2789.5 (m), 1746.5 (w), 1624.6 (w), 1490.5 (s), 1336.0 (m), 1253.5 (s), 1196.9 (s), 1094.4 (m), 1044.3 (m), 988.3 (m), 852.4 (s), 655.1 (s), 619.7 (s), 482.8 (m). Anal. Calcd for C$_{52}$H$_{76}$N$_8$Al$_4$: C, 67.80; H, 8.32; N, 12.17. Found: C, 67.01; H, 8.25; N, 12.43.

*[(μ^1,μ^1-dmbzim)(μ-Al)^{i}Bu$_2$]$_4$ (**11**).* A solution of Al^{i}Bu$_3$ (0.20 g, 1.08 mmol) in 15 mL of benzene was slowly added to a stirred solution of 5,6-dimethylbenzimidazole (0.15 g, 1.02 mmol) in 15 mL of benzene. The reaction mixture was stirred for 6 h at ambient temperature, concentrated, and stored at 4 °C. Once the compound crystallized, it was isolated by cannula filtration and dried under dynamic vacuum. Yield: 0.25 g, 86%. ^{1}H NMR (CDCl$_3$): δ 7.25 (s, 2H, Ar−*H*), 7.21 (s, 1H, Ar−*H*), 2.32 (s, 3H, Ar−C*H*$_3$), 1.71 (m, 2H, Al−CH$_2$C*H*(CH$_3$)$_2$, 0.77 (d, 12H, Al−CH$_2$CH(C*H*$_3$)$_2$), 0.37 (d, 4H, Al−C*H*$_2$CH(CH$_3$)$_2$. ^{13}C NMR (CDCl$_3$): δ 147.90, 137.74, 133.32, 116.20, 28.21, 26.39, 22.08, 20.90. ^{27}Al (CDCl$_3$): δ 49.53. IR (ν_{max}/cm^{-1}): 3425.0 (w), 3029.6 (m), 2949.8 (s), 2863.2 (s), 1630.9 (w), 1586.7 (w), 1484.7 (s), 1403.5 (w), 1309.8 (w), 1262.3 (m), 1194.3 (m), 1011.4 (m), 954.7 (m), 852.8 (s), 675.3 (s), 485.7 (m), 433.6 (m). Anal. Calcd for C$_{68}$H$_{108}$N$_8$Al$_4$: C, 71.29; H, 9.50; N, 9.78. Found: C, 70.84; H, 9.31; N, 9.57.

*[(μ^1,μ^1-tmbzim)(μ-Al)Me$_2$]$_4$ (**12**).* A solution of Me$_3$Al (0.07 g, 1.00 mmol) in 15 mL of benzene was slowly added to a stirred solution of 2,5,6-trimethylbenzimidazole (0.15 g, 0.94 mmol) in 15 mL of benzene. The reaction mixture was stirred for 6 h at ambient temperature. The solution was concentrated to 10 mL and stored under argon at 4 °C. Once the compound crystallized, it was isolated by cannula filtration and dried under dynamic vacuum. Yield: 0.18 g, 90%. ^{1}H NMR (CDCl$_3$): δ 7.56 (s, 2H, Ar−*H*), 2.32 (s, 6H, Ar−C*H*$_3$), 1.78 (s, 3H, Ar−C*H*$_3$), −0.28 (s, 6H, Al−C*H*$_3$). ^{13}C NMR (CDCl$_3$): δ 158.03, 138.45, 132.43, 115.83, 20.75, 15.89, −5.82. ^{27}Al (CDCl$_3$): δ 49.91. IR (ν_{max}/cm^{-1}) 2737.0 (s), 1453.8 (s), 1400.1 (s), 1301.3 (m), 1200.9 (m), 1001.1 (m), 860.8 (m), 678.8 (s), 588.7 (m), 442.2 (m). Anal. Calcd for C$_{48}$H$_{68}$N$_8$Al$_4$: C, 66.65; H, 7.92; N, 12.95. Found: C, 66.12; H, 7.69; N, 12.81.

*[(μ^1,μ^1-tmbzim)(μ-Al)Et_2]$_4$ (**13**).* A solution of Et_3Al (0.11 g, 1.00 mmol) in 15 mL of benzene was slowly added to a stirred solution of 2,5,6-trimethylbenzimidazole (0.15 g, 0.94 mmol) in 15 mL of benzene. The reaction mixture was stirred for 6 h at ambient temperature. The solution was concentrated to 10 mL and stored under argon at 4 °C. Once the compound crystallized, it was isolated by cannula filtration and dried under dynamic vacuum. Yield: 0.11 g, 90%. Mp: 290 °C. ^{1}H NMR ($CDCl_3$): δ 7.54 (s, 2H, Ar−*H*), 2.30 (s, 6H, Ar−CH_3), 1.79 (s, 3H, Ar−CH_3), 0.94 (t, 6H, Al−CH_2CH_3), 0.44 (q, 4H, Al−CH_2CH_3). ^{13}C NMR ($CDCl_3$): δ 157.66, 138.62, 132.56, 115.65, 20.61, 15.59, 8.89, 2.03. IR (ν_{max}/cm^{-1}): 2935.1 (s), 2864.1 (s), 1544.9 (w), 1555.1 (s), 1401.2 (s), 1303.2 (m), 1174.4 (w), 1001.7 (m), 856.8 (m), 820.5 (m), 646.3 (s), 451.8 (m). Anal. Calcd for $C_{56}H_{84}N_8Al_4$: C, 68.83; H, 8.66; N, 11.47. Found: C, 68.42; H, 8.34; N, 11.31.

*[(μ^1,μ^1-tmbzim)(μ-Al)^{i}Bu$_2$]$_4$ (**14**).* A solution of ^{i}Bu$_3$Al (0.20 g, 1.00 mmol) in 15 mL of benzene was slowly added to a stirred solution of 2,5,6-trimethylbenzimidazole (0.15 g, 0.94 mmol) in 15 mL of benzene. The reaction mixture was stirred for 6 h at ambient temperature. The solution was concentrated to 10 mL and stored under argon at 4 °C. Once the compound crystallized, it was isolated by cannula filtration and dried under dynamic vacuum. Yield: 0.20 g, 89%. ^{1}H NMR ($CDCl_3$): δ 7.51 (s, 2H, Ar−*H*), 2.33 (s, 6H, Ar−CH_3), 1.76 (s, 3H, Ar−CH_3), 1.53 (m, 2H, Al−$CH_2CH(CH_3)_2$, 0.77 (d, 12H, Al−$CH_2CH(CH_3)_2$), 0.56 (d, 4H, Al−$CH_2CH(CH_3)_2$. ^{13}C NMR ($CDCl_3$): δ 157.87, 138.44, 132.41, 115.80, 28.26, 26.47, 24.38, 20.71, 16.04. IR (ν_{max}/cm^{-1}): 3048.8 (w), 2948.7 (s), 2866.2 (s), 1629.6 (w), 1546.0 (w), 1455.8 (s), 1400.3 (s), 1307.7 (m), 1173.4 (m), 1059.3 (m), 1010.5 (m), 857.1 (m), 819.5 (m), 680.3 (s), 454.8 (s). Anal. Calcd for $C_{72}H_{116}N_8Al_4$: C, 71.96; H, 9.73; N, 9.32. Found: C, 71.44; H, 9.57; N, 9.12.

■ ASSOCIATED CONTENT

Ⓢ Supporting Information

Details of X-ray crystallography collection and refinement, figures of molecular and crystal structures for complexes **2**, **7**, **11**, and **14**, ^{1}H and ^{13}C NMR spectra for complexes **2**, **3**, **6**, **7**, **9**, **10**, and **12**−**14**, and crystallographic information files in CIF format. This material is available free of charge via the Internet at http://pubs.acs.org.

■ AUTHOR INFORMATION

Corresponding Author

*E-mail: mamund2@uaem.mx.

Notes

The authors declare no competing financial interest.

■ ACKNOWLEDGMENTS

The authors are grateful for financial support from CONACyT (Grants 56450, 54151, and 155247).

■ REFERENCES

(1) Rufino-Felipe, E.; Munoz-Hernandez, M.-A. *Chem. Commun.* **2011**, *47*, 3210−3212.
(2) Gutsche, C. D. *Acc. Chem. Res.* **1983**, *16*, 161−170.
(3) *Calixarenes, A Versatile Class of Macrocyclic Compounds*; Kluwer Academic Publishers: London, 1991; Vol. 3.
(4) Gutsche, C. D. *Calixarenes, An Introduction*, 2nd ed.; Royal Society of Chemistry: Cambridge, U.K., 2008.
(5) Stang, P. J.; Cao, D. H.; Chen, K.; Gray, G. M.; Muddiman, D. C.; Smith, R. D. *J. Am. Chem. Soc.* **1997**, *119*, 5163−5168.
(6) Diederich, F. *Cyclophanes*; Royal Society of Chemistry: Cambridge, U.K., 1991.
(7) Atwood, J. L. *Inclusion Phenomena and Molecular Recognition*; Plenum Press: New York, 1990.
(8) Vögtle, F.; Weber, E. *Host Guest Complex Chemistry: Macrocycles: Synthesis, Structures, Applications*; Springer: Berlin, 1985.
(9) König, B.; Fonseca, M. H. *Eur. J. Inorg. Chem.* **2000**, 2303−2310.
(10) Rauter, H.; Hillgeris, E. C.; Erxleben, A.; Lippert, B. *J. Am. Chem. Soc.* **1994**, *116*, 616−624.
(11) Lai, S.-W.; Chan, M. C. W.; Cheung, K.-K.; Peng, S.-M.; Che, C.-M. *Organometallics* **1999**, *18*, 3991−3997.
(12) Khutia, A.; Sanz Miguel, P. J.; Lippert, B. *Chem.—Eur. J.* **2011**, *17*, 4205−4216.
(13) Khutia, A.; Sanz Miguel, P. J.; Lippert, B. *Chem.—Eur. J.* **2011**, *17*, 4195−4204.
(14) Sathiyendiran, M.; Tsai, C.-C.; Thanasekaran, P.; Luo, T.-T.; Yang, C.-I.; Lee, G.-H.; Peng, S.-M.; Lu, K.-L. *Chem.—Eur. J.* **2011**, *17*, 3343−3346.
(15) Weiss, A.; Barba, V.; Pritzkow, H.; Siebert, W. *J. Organomet. Chem.* **2003**, *680*, 294−300.
(16) Barba, V.; Hopfl, H.; Farfan, N.; Santillan, R.; Beltran, H. I.; Zamudio-Rivera, L. S. *Chem. Commun.* **2004**, 2834−2835.
(17) Barba, V.; Villamil, R.; Luna, R.; Godoy-Alcántar, C.; Höpfl, H.; Beltran, H. I.; Zamudio-Rivera, L. S.; Santillan, R.; Farfán, N. *Inorg. Chem.* **2006**, *45*, 2553−2561.
(18) Barba, V.; Hernández, R.; Höpfl, H.; Santillan, R.; Farfán, N. *J. Organomet. Chem.* **2009**, *694*, 2127−2133.
(19) Atwood, D. A.; Harvey, M. J. *Chem. Rev.* **2001**, *101*, 37−52.
(20) Huang, X.-C.; Zhang, J.-P.; Chen, X.-M. *J. Am. Chem. Soc.* **2004**, *126*, 13218−13219.
(21) Wolff, S. K.; Grimwood, D. J.; McKinnon, J. J.; Turner, M. J.; Jayatilaka, D.; Spackman, M. A. *CrystalExplorer*, version 3.0; University of Western Australia: Crawley, Western Australia, 2012.
(22) Turner, M. J.; McKinnon, J. J.; Jayatilaka, D.; Spackman, M. A. *CrystEngComm* **2011**, *13*, 1804−1813.
(23) Steiner, T. *Angew. Chem., Int. Ed.* **2002**, *41*, 48−76.
(24) Prins, L. J.; Reinhoudt, D. N.; Timmerman, P. *Angew. Chem., Int. Ed.* **2001**, *40*, 2382−2426.
(25) Hunter, C. A.; Lawson, K. R.; Perkins, J.; Urch, C. J. *J. Chem. Soc., Perkin Trans. 2* **2001**, 651−669.
(26) Meyer, E. A.; Castellano, R. K.; Diederich, F. *Angew. Chem., Int. Ed.* **2003**, *42*, 1210−1250.
(27) Phillips, M. A. *J. Chem. Soc.* **1928**, 2393−2399.
(28) Sheldrick, G. M. *SMART*; Bruker AXS, Inc.: Madison, WI, 2000.
(29) Sheldrick, G. M. *SAINT-Plus*, version 6.0; Bruker AXS, Inc.: Madison, WI, 2000.
(30) Sheldrick, G. M. *SHELXTL*, version 6.10; Bruker AXS, Inc.: Madison, WI, 2000.
(31) *Diamond: Crystal and Molecular Structure Visualization Crystal Impact*; K. Brandenburg & H. Putz GbR, Bonn, Germany, 2004.
(32) *Mercury CSD 3.0—new features for the visualization and investigation of crystal structures*: Macrae, C. F.; Bruno, I. J.; Chisholm, J. A.; Edgington, P. R.; McCabe, P.; Pidcock, E.; Rodriguez-Monge, L.; Taylor, R.; Streek, J. v. d.; Wood, P. A. *J. Appl. Crystallogr.* **2008**, *41*, 466−470.
(33) Persistence of Vision Pty. Ltd. Persistence of Vision (TM) Raytracer, Williamstown, Victoria, Australia, 2004, http://www.povray.org/.